Buletinul Ştiinţific al Universităţii "Politehnica" din Timisoara, ROMÂNIA
Seria CHIMIE ŞI INGINERIA MEDIULUI
Chem. Bull. "POLITEHNICA" Univ. (Timişoara) *Volume 53(67), 1-2, 2008*

Textural Characterization of a New Iron-Based Ammonia Synthesis Catalyst

I. Siminiceanu[*], I. Lazau[**], Z. Ecsedi[**], L. Lupa[**], C. Burciag[***]

[*] Technical University "Gh.Asachi" of Iaşi, Bd. Mangeron 71, Iaşi 700050, Romania E-mail: isiminic@ch.tuiasi.ro

[**] University "Polytechnica" of Timisoara, Faculty of Industrial Chemistry and Environmental Engineering, Piata Victoriei Nr 2, Timisoara 300062, Romania

[***] SC AMURCO SRL Bacau, Str. Chimiei Nr.1, Bacau 600289, Romania ,Tel 0040-234575440

Abstract: A new iron- based promoted catalyst designed to be charged into the industrial radial- axial flow reactor was investigated in an Accelerated Surface Area and Porosity Analyzer- Micrometrics ASAP 2020. The primary experimental curve was identified as an adsorption/ desorption isotherm of type IV with H1 hysteresis. The main textural parameters (surface area, pore volume / porosity, pore size distribution (PSD) and average pore diameter) have been assessed usind six calculation methods : Langmuir model, BET equation, Single point method, t- Plot method, BJD adsorption, and BJH desorption. The surface area was between 12.33 m^2/g (Single point method) and 17.48 m^2/g (Langmuir model). From BET surface area the t- Plot has shown that about 9% was due to micro- pores. The average pore diameter derived from BJH adsorption model was of 16.72 nm. The determined parameters predict a better activity of the new catalyst compared to the traditional one.

Keywords: iron catalyst**,** surface area, porosity, pore size distribution, ASAP- 2020.

1. Introduction

It is estimated that without ammonia produced by the industrial process only 40% of the current global population could be nourished [1]. Ammonia was obtained for the first time by synthesis from elements in the Fritz Haber's laboratory at the University of Karlsruhe on July 2, 1909 at a rate of 80 g per hour [2]. Today is produced in industrial plants of over 1000 tons per day. The biggest plant will be put into operation in December 2010 in Saudi Arabia, based on *Mega Ammonia* technology, with a production capacity of 3300 tons/ day. The world production in 2006 was of 124 Mt [3]. Romania produced 1.05 Mt in the same year, the 6th in Europe after Russia, Ukraine, Germany, Poland and Netherlands. The actual production capacity of Romania is of about 3 Mt/ year, but the existing plants must be revamped, the processes must be improved in order to survive the market competition and to produce at their full capacity.

The major objective of the ammonia process development during the last decades was to reduce the energy input per unit mass of ammonia (GJ/t). Since the years 1930', when steam reforming of hydrocarbons was introduced as source of hydrogen for ammonia production, the specific energy consumption decreased from 85 GJ/t to about 29 GJ/t in the Lurgi- Ammonia Casale MEGAMMONIA process [4]. Even so, more then 1% of the total global energy consumption is currently used for ammonia production [5].Therefore, further improvements to the current technology could have a significant impact on the conservation of fossil fuels. Consequently, a continuous effort must be made to improve each step of the ammonia production process. The process has three main steps: raw synthesis gas production from natural gas by steam reforming, purification of synthesis gas (carbon monoxide shift conversion, carbon dioxide removal, final purification by methanation), and the synthesis loop. The synthesis loop includes compression, synthesis, separation of ammonia by refrigeration, and recirculation of unconverted gas. The contribution of the synthesis loop to the total energy input is of about 15% (4.6 GJ/t). The decrease of the pressure in the synthesis converter from 150- 300 bar to less than 100 bar has been analyzed by simulation [6]. Further, to reduce the compression and recirculation energy input a novel radial- axial flow reactor (RAR) has been proposed and implemented [7, 8]. Nevertheless, the reduction of pressure induces a negative effect: the synthesis rate decreases, and the conversion per pass becomes even less then 20%. Consequently, the synthesis catalyst must be improved to attenuate the negative effect of pressure decrease.

The goal of the present work was to assess the main textural parameters of a new iron- based ammonia synthesis catalyst, designed to be charged into the industrial radial- axial flow reactor of the ammonia plant in SC AMURCO SRL Bacau.

2. Experimental

The textural characteristics of the ammonia synthesis catalyst were determined from nitrogen adsorption/desorption isotherms at 77 K using a Micrometrics ASAP 2020 Surface Area and Porosity Analyzer. Before analyses the samples were automatically

degassed under vacuum for about six hours. The sample mass was of 8.8757 g. The cold free space 46.7856 cm^3 and the warm free space of 15.7232 cm^3 (measured).

The catalyst tested was an iron- based porous material containing "textural" promoters such as oxides of aluminum, calcium, magnesium, and silicon as well as "electronic" promoters such as potassium- oxygen compounds. The textural promoters are characterized by their ability to form substitutional spinel-type ternary oxides within the inverse spinel structure of the host precursor magnetite. It is estimated that the structural promoters increase the specific surface area of the activated catalyst, which varies from a few m^2/g for unpromoted oxide up to about 18 m^2/g for a promoter concentration of 3 % [2]. In addition, they stabilize the initially- formed iron sponge structure against recrystallization/sintering by forming thin surface film of textural promoters, especially of alumina. The new catalyst to be introduced into the radial- axial flow reactor of the ammonia plant in AMUR Co Bacau has also a different granulometric spectrum (Table 1). Most particles have diameters between 1 and 3 mm, whereas the traditional catalyst had 3 - 8 mm.

TABLE 1. Granulometry of the tested catalyst

Class, mm	*Mass percent, %*	*Average diameter, mm*
d > 3.15	*0.50*	
3.15> d < 2.5	*16.50*	$d_{av} = \Sigma d_i x_i = 2.3113$
2.5 >d <2.0	78.45	
2.0> d < 1.0	*4.25*	
1.0> d < 0.8	*0.10*	
0.8 > d	*0.20*	

Other measured properties: particle density using a gravity bottle was 4.2857 g/ cm^3 and bulk density 2.3530 g/ cm^3.

3. Results and discussion

A typical experimental adsorption/ desorption isotherm of nitrogen on the ammonia synthesis catalyst is shown in Figure 1. The first point of discussion is the identification of the type of isotherm.

The forms of the isotherms and hysteresis loops have been subjected to a classification initially proposed by Brunauer et al. [10], the so called BDDT classification, and then taken up by IUPAC [11,12,13]. Four types of isotherms out of the six proposed by IUPAC are commonly encountered [11]: I, II, IV, and VI. Similarly, the hysteresis loops, corresponding to mesoporous systems, have been classified, in terms of their forms, into four categories: H1, H2, H3, and H4. The comparison of the experimental isotherm in Fig.1 with the typical IUPAC forms published in reference books [11] leads to the conclusion that it is of the type IV with H1 hysteresis. This means that the tested catalyst is mostly mesoporous. The classification of pores into micro- (with diameter less then 2 nm), meso- (2- 50 nm), and macro- pores (larger then 50 nm), proposed by Dubinin [14], is now unanimously accepted [11, 12, 13]. The hysteresis H1 has a narrow loop with two branches almost vertical and parallel. This form of hysteresis is often associated with adsorbents made up of agglomerates leading to narrow pore size distribution (PSD).

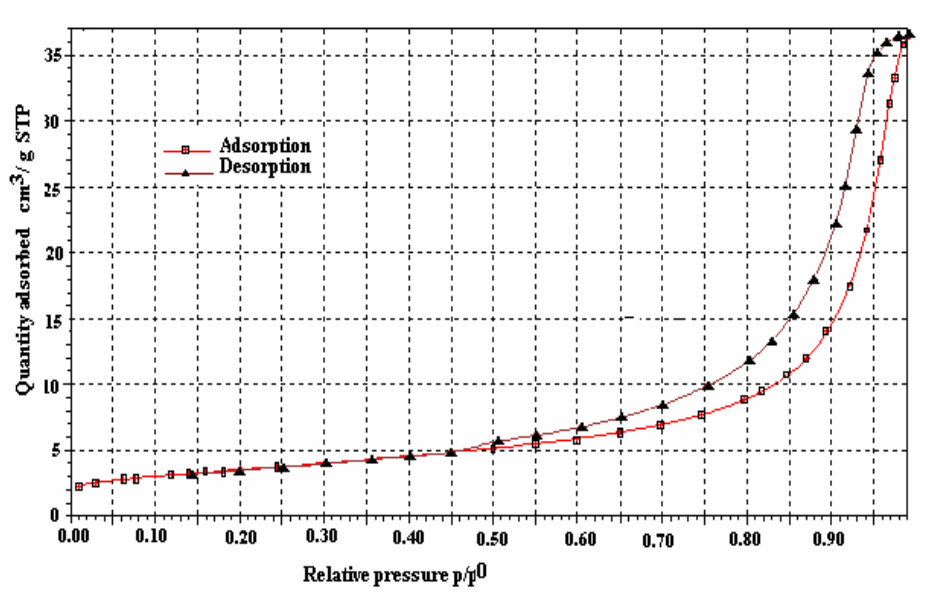

Figure1. Adsorption isotherm (linear plot)

The interpretation of adsorption-desorption isotherms provides a great deal of information on the texture of the adsorbent. The main parameters that can be assessed are:

- specific surface area (S, m^2/g);
- specific pore volume (v_p, cm^3/g);
- porosity (ε, cm^3/cm^3);
- pore size distribution (PSD);
- the average pore size (d_{av}).

In addition, qualitative information on the structure (pore shape, interconnection) can be obtained.

There are many mathematical models to calculate the above textural parameters from the experimental isotherms. Some of them are listed in the Table 2.

TABLE 2. Calculation models/methods for textural parameters

P/P^0 range	Mechanism	Calculation model*
10^{-7}- 0.02	Micropore filling	DFT, GCMC, HC, SF, DA, DR
0.01- 0.10	Sub- monolayer formation	DR
0.05- 0.30	Monolayer complete	BET, LA
>0.10	Multilayer formation	t- Plot, α_S
>0.35	Capillary condensation	BJH, DH
0.10- 0.50	Capillary filling	DFT, BJH

- DFT= Density Functional Theory, GCMC= Grand Canonical Monte Carlo, HK= Horvath- Kawazoe, SF= Saito- Foley, DA= Dubinin- Astakhov, DR= Dubinin- Radushkevic, BET= Brunauer- Emmett- Teller, LA= Langmuir, t- Plot= statistical thickness method, α_S= alpha- S (Sing) method, BJH= Barrett- Joyner- Halenda method, DH= Dollimore- Heal.

The methods used in this work (LA, BET, Single point, t-Plot, BJH) are subsequently discussed.

The Langmuir model

Although the term "adsorption" was introduced in the literature in 1881 by Heinrich Kayser (1853-1940), the founder of the adsorption theory was Irving Langmuir (1881-1957), who was a Nobel laureate in Chemistry (1932). He established the best known "Langmuir isotherm" [15]:

$$V_a/ v_m = \theta = K P/ (1+ K P) \qquad (1)$$

which can be linearized under forms (2) and (3):

$$1/ v_a = 1/ v_m + 1/ v_m K P \qquad (2)$$

$$(P/P_0)/ v_a = 1/ v_a K P_0 + (P/P_0)/v_m \qquad (3)$$

By representing the equation (3) with v_a and the relative pressure (P/P_0) from the experimental curve, the adsorbed volume of a monolayer v_a can be obtained from the slope of the Langmuir plot (Fig.2). Then, the specific surface area S is calculated with the formula (4):

$$S = (N_A \, a \, v_m \times 10^{-20})/ m_s \, v_M = 4.35 \, v_m \qquad (4)$$

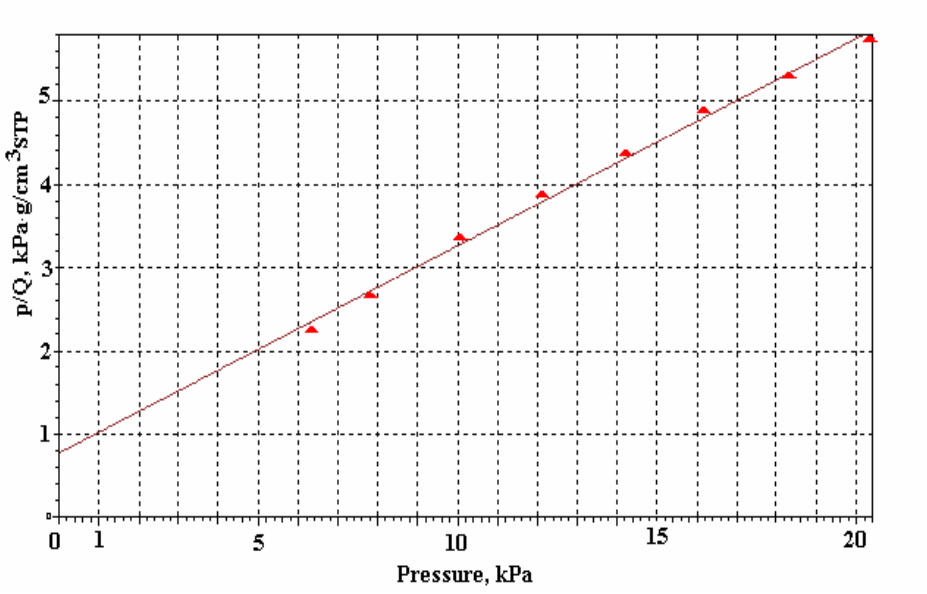

Figure 2. Langmuir surface area plot

The LA model is based on the monolayer assumption. Therefore, the surface area obtained with the formula (4) is an overestimation of the actual surface area (Table 3).

Nevertheless, the Langmuir equation is suitable for chemical adsorption as well as for physical adsorption on some micro-porous materials [13].

The Brunauer- Emmett- Teller(BET) model

The BET model [16] is an extension of the Langmuir theory from the monolayer molecular adsorption to the multilayer adsorption. The LA model is applied for each layer. The final form of the BET linear equation is:

$$(P/P_0) / v_a (1-P/P_0) = 1 /v_m C + (P/P_0) (C- 1) / v_m C \quad (5)$$

where C is the BET constant, specific to each system. A straight line $P/ v_a(P_0- P)$ as a function of P/P_0 can be used to obtain:

$$v_m = 1/ (A + B) \text{ and } C = 1+ (B/A),$$

where A is the ordinate at the origin and B is the gradient of the straight line. This is the so called "BET plot. The surface area is then calculated with formula (4).

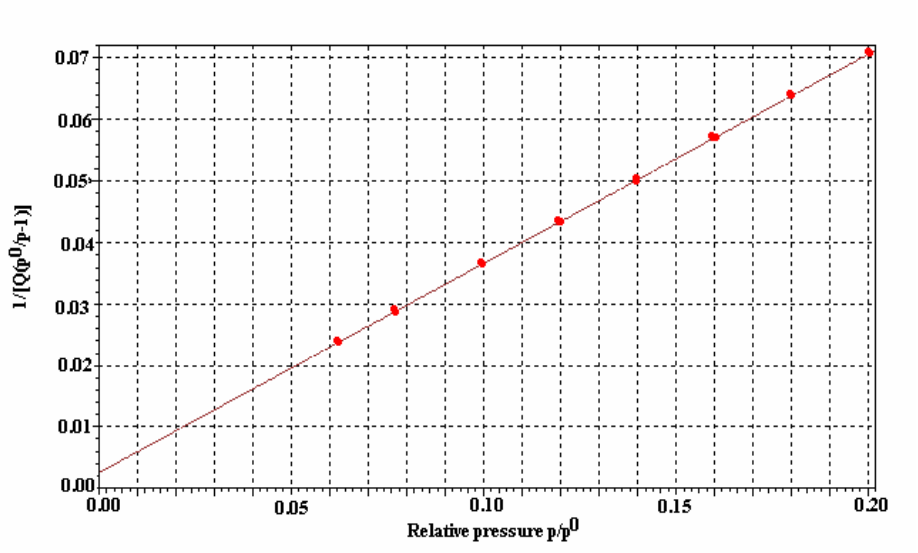

Figure 3. BET surface area plot

Generally, for isotherms of the types II and IV for big mesopores the BET equation is well verified in the range $0.05 < P/P_0 < 0.35$. For the isotherm IV and small mesopores the linearity is maintained only in range $0.05 < P/P_0 < 0.20$, and the surface area is slightly overestimated (Table 3).

TABLE 3. Calculated textural parameters

Method	Surface area, m^2/g	Pore volume, cm^3/g	Average pore diameter, nm
Langmuir	17.4795	-	-
BET	12.6917		
Single point, at $P/P_0= 0.2$	12.3279	0.05632	17.75065
t- Plot	Micropore 1.1438 External 11.5479	Micropore: 0.000432	-
BJH adsorption	13.5640	0.056716	16.7257
BJH desorption	16.6438	0.056537	13.5875

Single- point estimation

The method takes into consideration only the so called "point B" , the intersection of initial concave curve with the linear segment of the S shaped isotherm. On the isotherm in Fig. 1 the point B is at $P/P_0 = 0.2004$. Taking v_a directly from the isotherm, the "single point surface area" is 12. 3279 m^2/g , very close to BET surface area (Table 3).

t- Plot model

The t- Plot method is attributed to Lippens and De Boer [17,18]. They proposed the plotting of the nitrogen adsorbed volume (v_a) at different P/P_0 values as a function of the layer thickness (t). The resulting curve is compared with the experimental isotherm in the form of t- plot (Figure 4.).

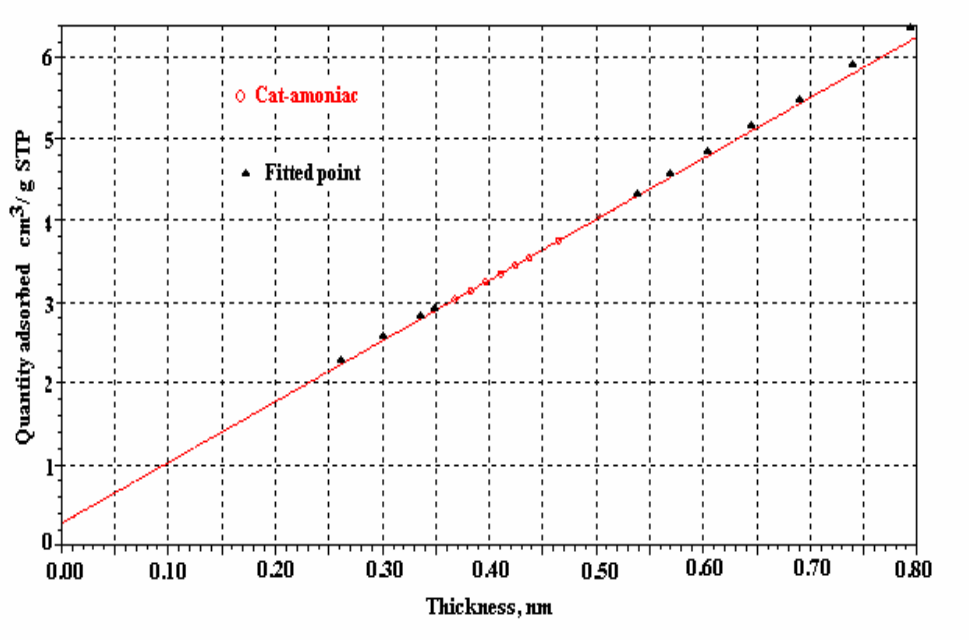

Figure 4. Harkins and Jura t- plot

The linear range lies between monolayer and capillary condensation. The slope of the t- plot, v_a/t, is equal to the "external" area, i.e. the area of those pores which are not micro- pores (meso-, macro-, and exterior surface of the particle). These pores are able to form multilayers whereas micropores, which have already been filled by the adsorption fluid, cannot contribute further to the adsorption process. The model allows separating the micropores from meso-, macro-, and outside surface. This separation is illustrated by the equation (6):

$$v_a\,(P/P_0) = v_a\,(\text{micro}) + k\,S_{ex}\,t\,(P/P_0) \qquad (6)$$

The layer thickness t from (6) is replaced with t from the equation of Harkins and Jura [19]:

$$t = [13.99/\,(0.34 - \log P/P_0)\}^{1/2} \qquad (7)$$

For pore size evaluation the equation of Halsey is preferred [20]:

$$t = 3.54\,[\,5/\log\{P/P_0\}]^{1/3} \qquad (8)$$

The model of Lippins and De Boer is valid only in a narrow range of relative pressure. It is recommended to initially select $0.20 < P/P_0 < 0.50$, and subsequently to adjust it to find the best linear plot. The results for the ammonia synthesis catalyst are represented in Figure 4, and included in Table 3. From the slope of the linear t- plot results S_{ex} = 11.5479 m^2/ g. The surface of micropores (= 1. 1438 m^2/g) results from the ordinate at origin. The sum of the two surfaces is exactly the BET surface (12.6917 m^2/g). The perfect linearity of t- plot at t = 0.35-0.60 nm. The surface of micropores is only 9.01 % from the total. The ammonia synthesis catalyst is mostly mesoporous.

The BJH method

Barrett, Joyner and Halenda [21] proposed a calculation method for the distribution curves of the pore volume ($dV_p/ d d_p$, cm^3/ g nm) or of the surface area ($dS/ d d_p$, m^2/g nm) as a function of pore diameter from nitrogen adsorption- desorption data. From the surface distribution the cumulative BJH surface area is derived:

$$S_{cum} = 2\,\Sigma v_{pi}/\,\Sigma r_{pi} \qquad (10)$$

The cylindrical pore radius (r_p) is connected to the thickness of adsorbed layer (t) and the meniscus radius (r_K) given by the Kelvin ecuation:

$$r_p = t + r_K = t - 4.5/\log(P/P_0) \qquad (11)$$

where the thickness t is calculated with the Halsey equation (8). Starting from the isotherm $v_a = f(P/P_0)$ it's possible to correlate every v_a value to r_p and to obtain a function $v_a = f(r^p)$ which gives the necessary gas volume to fill by condensation all the pores with radius < r_p. The derivative of this function (dv_a/dr_p) gives the pore volume repartition as function of r_p. Knowing the form of the pores it is possible also to obtain the surface area distribution of pores (dS/dr_p) as a function of r_p.

The BJH distribution curve obtained for the ammonia synthesis catalyst (Figure 5) led to a cumulative adsorption surface of 13.564 m^2/g and an average pore diameter of 16.7257 nm (Table 3). The fact that $S_{cum} > S_{BET}$ proves the existence of many bottle- shaped pores [11, 22]. This form favoures the small diameters and, for a given volume, the calculated area is overestimated. It must be also remarked that the BJH desorption distribution leads to an underestimated average pore diameter. This may be due to the fact that the thermodynamic gas- solid equilibrium is less stable at desorption when such non- cylindrical pores are involved.

All the average pore diameters were calculated with the formula (12), considering cylindrical form:

$$d_{av} = 4\,V_p/S \qquad (12)$$

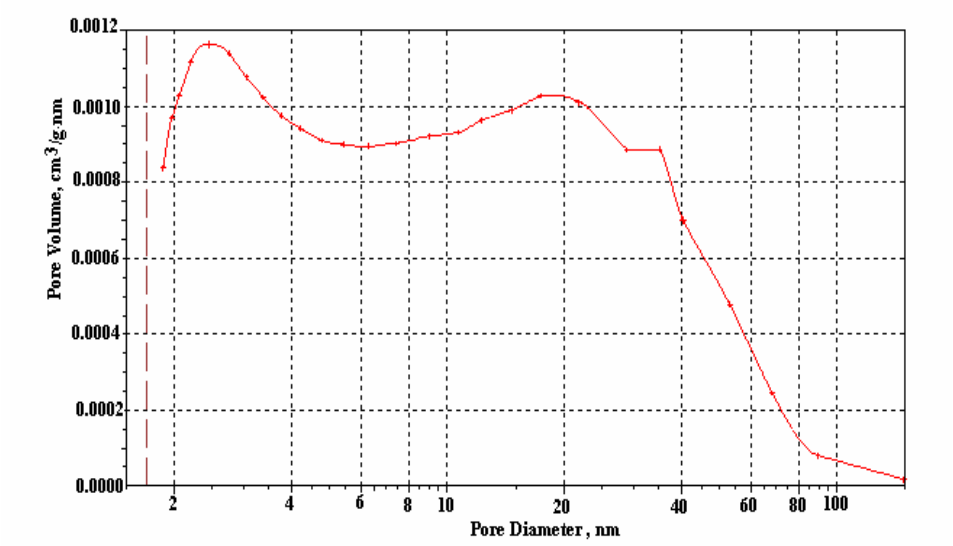

Figure5. BJH adsorption dV/dD pore volume: Halsey plot with FAAS correction

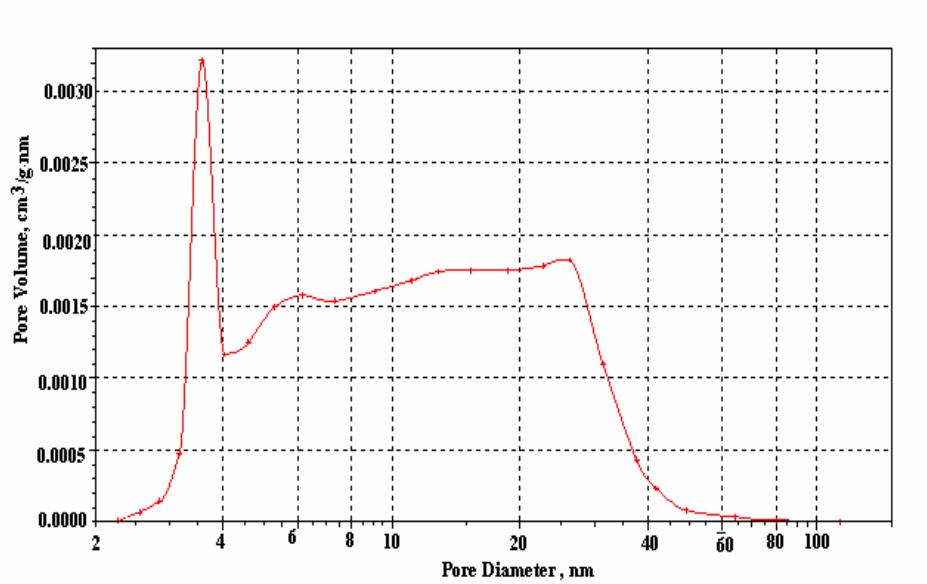

Figure 6. BJH desorption dV/dD pore volume: Halsey plot with FAAS correction

4. Conclusions

The industrial manufacture of ammonia by synthesis is a process of vital importance for the survival of a growing population. But the current technology is highly energo-intensive. A short term objective is to decrease the energy consumption to less than 30 MJ/t. The improvement of the ammonia synthesis loop by the introduction of the radial-axial flow reactor at medium pressure must be accompanied by the use of a more active catalyst.

The new iron- based promoted catalyst designed to be charged into the industrial radial- axial flow reactor was investigated in an Accelerated Surface Area and Porosity Analyzer-Micrometrics ASAP 2020. The primary experimental curve was identified as an adsorption/ desorption isotherm of type IV with H1 hysteresis.

The main textural parameters (surface area, pore volume / porosity, pore size distribution (PSD) and average pore diameter) have been assessed using six calculation methods : Langmuir model, BET equation, Single point method, t- Plot method, BJD adsorption, and BJH desorption. The calculated values of the surface area were between 12.33 m^2/g (Single point method) and 17.48 m^2/g (Langmuir model). From BET surface area the t- Plot has shown that about 9% was due to micro- pores. The average pore diameter derived from BJH adsorption model was of 16.72 nm. The determined parameters predict a better activity of the new catalyst compared to the traditional one.

Notation

a, area occupied by an adsorbed gas molecule (0.162 $Å^2$ for nitrogen);

d_{av}, average pore diameter, nm;
K, equilibrium constant of adsorption;
N_A, Avogadro's number;
m_s, mass of adsorbent sample, g;
P, equilibrium pressure, MPa;
P_0, saturated vapour pressure, MPa;
r_K, meniscus Kelvin radius, nm;
S, specific surface area, m^2/ g;
v_a, adsorbed volume at equilibrium of adsorption , cm^3/ g, at standard T and P (STP);
v_m, adsorbed volume in a monolayer , at STP;
v_M, molar volume, 22.414 cm^3/ mol at STP.
V_p, pore volume, cm^3/g
t, layer thickness, nm;
T, temperature, K.

REFERENCES

1. Appl, M., Ammonia: Production Principles and Industrial Practice, Wiley- VCH, New York, **1999**.
2. Jennings, J.R. (Editor), Catalytic Ammonia Synthesis: Fundamentals and Practice, Plenum Press, New York, **1991**.
3. The USGS Mineral Resources Program, **2007**, http://minerals.usgs.gov/
4. Filippi, E., The Mega Ammonia Process: The Newest Trend in the Ammonia Industry, in: Proceedings of AFA 18th International Annual Technical Conference & Exhibition, 5- 7 July **2005,** Casablanca.
5. Jacobsen, C.J.H., Dahl, S., Boisen, A., Clausen, B.S., Topsoe, H., Logadottir, A., Norskov, J.K., *J. Catal.*, **2002**, 205(2), pp. 283- 287.
6. Siminiceanu, I., Petrila, C., Pop, A., *Chem. Tech.*, **1991**, 43, pp. 257- 261.
7. Panahandeh, M.R., Fathikaljahi, J., Taheri, M., *Chemical Engineering & Technology*, **2003**, 26, pp. 666-671.
8. Zardi, F., Bonvin, D., *Chem. Eng. Sci.*, **1992**, 47, pp. 2523- 2528.
9. Nielsen, A., An Investigation on Promoted Iron Catalysts for the Synthesis of Ammonia, 3rd Edition, Jul. Gjellerups Forlag, Copenhagen, **1968**.
10. Brunauer, S., Deming, L., Deming, W., Teller, E., *J. Amer. Chem. Soc.*, **1940**, 62, pp. 1723- 1727.
11. Uzio, D., Textural Characterization of Catalysts, in: Lynch J. (Editor), Physico-Chemical Analysis of Industrial Catalysts, Edition Technip, Paris, **2001**, pp. 5 - 26.
12. Toth, J., Adsorption: Theory, Modeling, and Analysis, Marcel Dekker, New York, **2002**.
13. Dabrowski, A., *Advances in Colloid and Interface Science*, **2001**, 93, pp. 135-224.
14. Dubinin, M.M., *Pure Appl. Chem.*, **1966**, 10, pp. 309- 313.
15. Langmuir, I., *J. Amer. Chem. Soc.*, **1916**, 38, pp. 2263.
16. Brunauer, S., Emmett, P.H., Teller, E., *J. Amer. Chem. Soc.*, **1938**, 60, pp. 309.
17. Lippens, B.C., de Boer, J.H., *J. Catal.*, **1965**, 4, pp. 319.
18. De Boer, J.H., Lippens, B.C., Linsen, B.G., Broekhoff, J.C.P., van den Heuvel, A., Osinga, Th. J., *J. Colloid Interface Sci.*, **1966**, 21, pp. 404.
19. Jura, G., Harkins, W.D., *J. Amer. Chem. Soc.*, **1944**, 66, pp. 1856.
20. Halsey, G.D., *J. Chem. Phys.*, **1948**, 16, pp. 931.
21. Barrett, E.P., Joyner, L.G., Halenda, P.P., *J. Amer. Chem. Soc.*, **1951**, 73, pp. 373.
22. Choma, J., Jaromec, M., *Applied Surface Science*, **2007**, 253(13), pp. 5587- 5590.